Hepatology Research 2009; **39**: 805–813 doi: 10.1111/j.1872-034X.2009.00541.x

Original Article

Matrix metalloproteinase inhibitor, CTS-1027, attenuates liver injury and fibrosis in the bile duct-ligated mouse

Alisan Kahraman,[1,2] Steven F. Bronk,[1] Sophie Cazanave,[1] Nathan W. Werneburg,[1] Justin L. Mott,[1] Patricia C. Contreras[3] and Gregory J. Gores[1]

[1]*Miles and Shirley Fitterman Center for Digestive Diseases, Division of Gastroenterology and Hepatology, Mayo Clinic College of Medicine, Rochester, Minnesota,* [3]*Conatus Pharmaceuticals, San Diego, California, USA; and* [2]*Department of Gastroenterology and Hepatology, University Clinic Essen, Duisburg-Essen University Duisburg-Essen, Germany*

Aim: Excessive matrix metalloproteinase (MMP) activity has been implicated in the pathogenesis of acute and chronic liver injury. CTS-1027 is an MMP inhibitor, which has previously been studied in humans as an anti-arthritic agent. Thus, our aim was to assess if CTS-1027 is hepato-protective and anti-fibrogenic during cholestatic liver injury.

Methods: C57/BL6 mice were subjected to bile duct ligation (BDL) for 14 days. Either CTS-1027 or vehicle was administered by gavage.

Results: BDL mice treated with CTS-1027 demonstrated a threefold reduction in hepatocyte apoptosis as assessed by the TUNEL assay or immunohistochemistry for caspase 3/7-positive cells as compared to vehicle-treated BDL animals ($P < 0.01$). A 70% reduction in bile infarcts, a histological indicator of liver injury, was also observed in CTS-1027-treated BDL animals. These differences could not be ascribed to differences in cholestasis as serum total bilirubin concentrations were nearly identical in the BDL groups of animals. Markers for stellate cell activation (α-smooth muscle actin) and hepatic fibrogenesis (collagen 1) were reduced in CTS-1027 versus vehicle-treated BDL animals ($P < 0.05$). Overall animal survival following 14 days of BDL was also improved in the group receiving the active drug ($P < 0.05$).

Conclusion: The BDL mouse, liver injury and hepatic fibrosis are attenuated by treatment with the MMP inhibitor CTS-1027. This drug warrants further evaluation as an anti-fibrogenic drug in hepatic injury.

Key words: apoptosis, cholestasis, liver fibrosis, matrix metalloproteinase

INTRODUCTION

LIVER FIBROSIS AND its end-stage sequela of cirrhosis represent a major worldwide health problem. Hepatic fibrosis is the result of an exuberant wound healing response resulting in excessive collagen deposition in the liver. Hepatic stellate cells are the major source of collagen in the diseased liver.[1] During liver injury, hepatic stellate cells undergo activation and transdifferentiation to myofibroblasts, which efficiently generate collagen I as part of their wound healing response.[1] These activated cells, interestingly, also secrete matrix metalloproteinases (MMP) which may degrade collagenous and non-collagenous substrates.[2] Usually, these potent proteases are held in check by the secretion of tissue inhibitors of metalloproteinases (TIMP)1 and 2.[2] However, excessive and prolonged MMP secretion can alter the hepatic scaffolding. This alteration of hepatic architecture results in further liver injury, which in turn elicits increased hepatic damage and fibrosis. It is this upregulated MMP activity which leads to a feed-forward damage response in liver injury. In particular, MMP-2, -3 and -9 are upregulated and thought to contribute to human liver disease.[3–5]

Inhibition of MMP activity is a potential strategy to minimize liver injury and reduce hepatic fibrogenesis. For example, inhibition of MMP activity by an MMP inhibitor, BB-94, blocks hepatocyte apoptosis and improves animal survival in a model of tumor necrosis factor-α (TNF-α) induced acute liver injury.[6] Genetic deletion of MMP-13, collagenase-3, attenuates hepatic

Correspondence: Dr Gregory J. Gores, Mayo Clinic College of Medicine, 200 First Street SW, Rochester, MN 55905, USA. Email: gores.gregory@mayo.edu
Received 26 March 2009; revised 9 April 2009; accepted 10 April 2009.

fibrogenesis in a cholestatic model of liver injury, the bile duct ligated (BDL) mouse.[7] These observations suggest MMP inhibition may be hepato-protective in liver injury. CTS-1027, N-hydroxy-4-([4-[4-chlorophenoxy] benzenesulfonyl] methyl)-2, 3, 5, 6-tetrahydropyran-4-carboxamide, is a reversible MMP inhibitor. It is an especially potent inhibitor of human MMP-2, -3, -8, -9, -12, -13 and -14 but not -1 or -7. The K_i for inhibiting these MMP is 9 nM or less. CTS-1027 appears to be selective for MMP and has little or no activity for other proteinases including caspases, the initiator and effector proteinases of apoptosis. This hydroxamate-based inhibitor has been studied in clinical trials as an anti-arthritic agent. The compound was well-tolerated and side-effects were generally mild, reversible and primarily limited to the musculoskeletal system. Thus, given its safety profile and selectivity in targeting MMP, CTS-1027 is an attractive agent to inhibit MMP as a potential hepato-protective agent. However, preclinical studies have not yet been reported addressing a potential hepato-protective effect, although CTS-1027 is currently in early phase 2 studies in hepatitis C virus patients.

In this study, we assessed the hepato-protective and anti-fibrogenic potential of CTS-1027 during cholestatic liver injury in a preclinical model, the BDL mouse. As compared to vehicle-treated control animals, administration of CTS-1027 attenuates hepatocyte apoptosis, liver injury and hepatic fibrosis.

METHODS

Animal models

THE CARE AND use of the animals for the following experiments were reviewed and approved by the Institutional Animal Care and Use Committee (IACUC) at Mayo Clinic. C57/BL6 wild-type (wt) mice (6–8 weeks of age, 20–25 g of bodyweight) were employed for these studies. Mice were maintained in a temperature-controlled (22°C), pathogen-free environment and fed a standard rodent chow diet and water ad libitum. For experimental procedures, mice were anesthetized with ketamine 60 mg/kg plus xylazine 10 mg/kg bodyweight by i.p. injection. After a midline upper-abdominal incision, the peritoneal cavity was opened, the abdominal wall retracted, and the common hepatic bile duct was double-ligated below the bifurcation and transected between the ligatures as previously described by us in detail.[8] Sham-operated mice, used as controls, also underwent similar laparotomy with exposure but without ligation of the common bile duct. The fascia and skin of the midline abdominal incision were closed with sterile surgical 5–0 sutures (Ethicon, Somerville, NJ, USA). Either CTS-1027 (Conatus Pharmaceuticals, San Diego, CA, USA) or the vector carboxymethylcellulose (CMC; Sigma-Aldrich Diagnostics, St Louis, MO, USA) were administered by gavage in a dose of 10 mg/kg bodyweight once a day. Drugs were prepared freshly on the day of the study. After 14 days of BDL and gavage, mice were re-anesthetized, euthanized by exsanguination as blood was obtained from the inferior vena cava for serum total bilirubin and alanine aminotransferase (ALT) determinations and the liver was removed, cut into small pieces and either snap-frozen in liquid nitrogen for storage at −80°C or fixed in freshly prepared 4% paraformaldehyde in phosphate-buffered saline for 48 h at 4°C for additional studies (vide infra). Liver tissue was also subjected to RNA extraction using the Trizol reagent (Invitrogen, Carlsbad, CA, USA). Serum bilirubin and ALT determinations were performed as previously described.[9]

Histopathology

For histological review of hematoxylin–eosin (HE)-stained liver sections by light microscopy (Nikon Eclipse Meta Morph ver. 5.0.7), the liver was diced into 5 mm × 5 mm sections, fixed in 4% paraformaldehyde for 48 h and then embedded in paraffin (Curtin Matheson Scientific, Houston, TX, USA). Tissue sections (4-μm) were prepared using a microtome (Reichert Scientific Instruments, Buffalo, NY, USA) and placed on glass slides. HE staining was performed according to standard techniques.

TUNEL assay and immunofluorescent identification of activated caspases 3 and 7

Apoptotic cells were quantitated by the terminal deoxynucleotidyl transferase-mediated dUTP nick-end labeling (TUNEL) assay which enzymatically labels free 3′-OH ends of damaged DNA with a fluorescently-labeled nucleotide as we have previously described in detail.[10] TUNEL-labeled cells (i.e. fluorescent nuclei) were quantified by counting the number of positive cells per high-power field (HPF). A total of 10 HPF were analyzed for each animal with excitation and emission wavelengths of 490 and 520 nm, respectively, using an inverted laser scanning confocal microscope (LSM 510; Carl Zeiss Micro-Imaging, Thornwood, NJ, USA) equipped with a 40× NA 1.4 lens and LSM 510 imaging software. Data were expressed as the number of

TUNEL-positive cells/10 HPF. Immunofluorescence analysis for activated caspases 3 and 7 was performed using a rabbit anti-active caspase 3 and 7 polyclonal antibody (BD Biosciences/Pharmingen, San Diego, CA, USA) recognizing a common neo-epitope shared by activated caspases 3 and 7 as we have previously described.[10] Secondary goat-antirabbit antibody conjugated to Texas Red-X (Invitrogen) was used for visualization of staining. The liver specimens were viewed by confocal microscopy using excitation and emission wavelengths of 543 and 568 nm, respectively. The number of caspase 3/7-positive cells was quantified per 10 HPF as described above for the TUNEL assay. Negative control slides were incubated with non-immune immunoglobulin under the same conditions.

Quantitative real time-polymerase chain reaction (qRT–PCR)

Total RNA was isolated from liver tissue using the Trizol reagent (Invitrogen). For each RNA sample, a 10-μg aliquot was reverse-transcribed into complementary DNA (cDNA) using random primers and Maloney murine leukemia virus (MMLV) reverse transcriptase (Invitrogen) as previously described in detail.[11] After the reverse transcription reaction, the cDNA template was amplified by real-time PCR with Plantinum Taq DNA polymerase (Invitrogen) using standard protocols. All amplified PCR products were confirmed by electrophoresis in 1% low-melting temperature agarose gel, stained with ethidium bromide and photographed using ultraviolet illumination. The expected bp PCR products were identified and the bands cut from the gel. Next, PCR products were eluted into Tris-HCl using a DNA elution kit (Qiagen, Valencia, CA, USA). The concentration of DNA in the extracted PCR product was measured spectrophotometrically at 260 nm (DU 4400; Beckman, Palo Alto, CA, USA) and converted to copies/μL. Extracted PCR products were prepared as standards. aRT–PCR was performed using a Light Cycler (Roche Diagnostics, Mannheim, Germany) and SYBR green as the fluorophore (Invitrogen) as previously described by us in detail.[12,13] PCR primers (all obtained from the Mayo DNA Synthesis Core Facility, Rochester, MN, USA) were as follows: α-smooth muscle actin (*α-SMA*) forward, 5′-ACT ACT GCC GAG CGT GAG AT-3′ and reverse, 5′-AAG GTA GAC AGC GAA GCC AG-3′ (yielding a 452-bp product); and *collagen 1α* (I) forward, 5′-GAA ACC CGA GGT ATG CTT GA-3′ and reverse, 5′-GAC CAG GAG GAC CAG GAA GT-3′ (yielding a 276-bp product).

Immunohistochemistry for *α-SMA* and determination of liver fibrosis by Sirius red staining

The sections were stained for *α-SMA* using a mouse monoclonal antibody (Neo Markers, Fremont, CA, USA). The sections were incubated with the primary antibody overnight at 4 °C. Negative control slides were incubated with non-immune immunoglobulin under the same conditions. Secondary reagents were obtained from the En Vision + System-HRP ready-to-use kit (Dako Cytomation, Carpinteria, CA, USA) and 3,3′-diaminobenzidine (DAB) chromogen solution was used for visualization by light microscopy. Finally, the tissue was counterstained with hematoxylin for 3 min. Liver fibrosis was quantified using Sirius red FSB (also called Direct Red 80) as described.[14] Direct red 80 and Fast green FCF (counterstain) were obtained from Sigma-Aldrich Diagnostics. Liver sections were stained and red-stained collagen fibers were quantified by digital image analysis as previously described by us in detail.[12]

Statistical analysis

All data are expressed as the mean ± standard error unless otherwise indicated. Differences between groups were compared using ANOVA for repeated measurements and post-hoc Bonferroni test to correct for multiple comparisons. $P < 0.05$ was considered to be statistically significant. All statistical analyses were performed using In-Stat Software.

RESULTS

Hepatocyte apoptosis is significantly reduced in the BDL mouse with CTS-1027 treatment

HEPATOCYTE APOPTOSIS IS a prominent feature of cholestatic liver injury and occurs in the bile duct ligated liver.[8] If an agent is to exert hepatoprotective properties, it should attenuate hepatocyte apoptosis. To examine the effects of the MMP inhibitor CTS-1027 on hepatic apoptosis, mice were subjected to BDL for 14 days. Liver specimens from BDL animals treated with vehicle demonstrated numerous clusters of apoptotic cells characterized by condensation of chromatin at the nuclear membrane and fragmentation of the cell into subcellular bodies in a background of altered hepatic micro-architecture (Fig. 1a). The MMP inhibitor significantly modified the extent of cell death from numerous clusters of apoptotic hepatocytes to reduced numbers of isolated apoptotic hepatocytes.

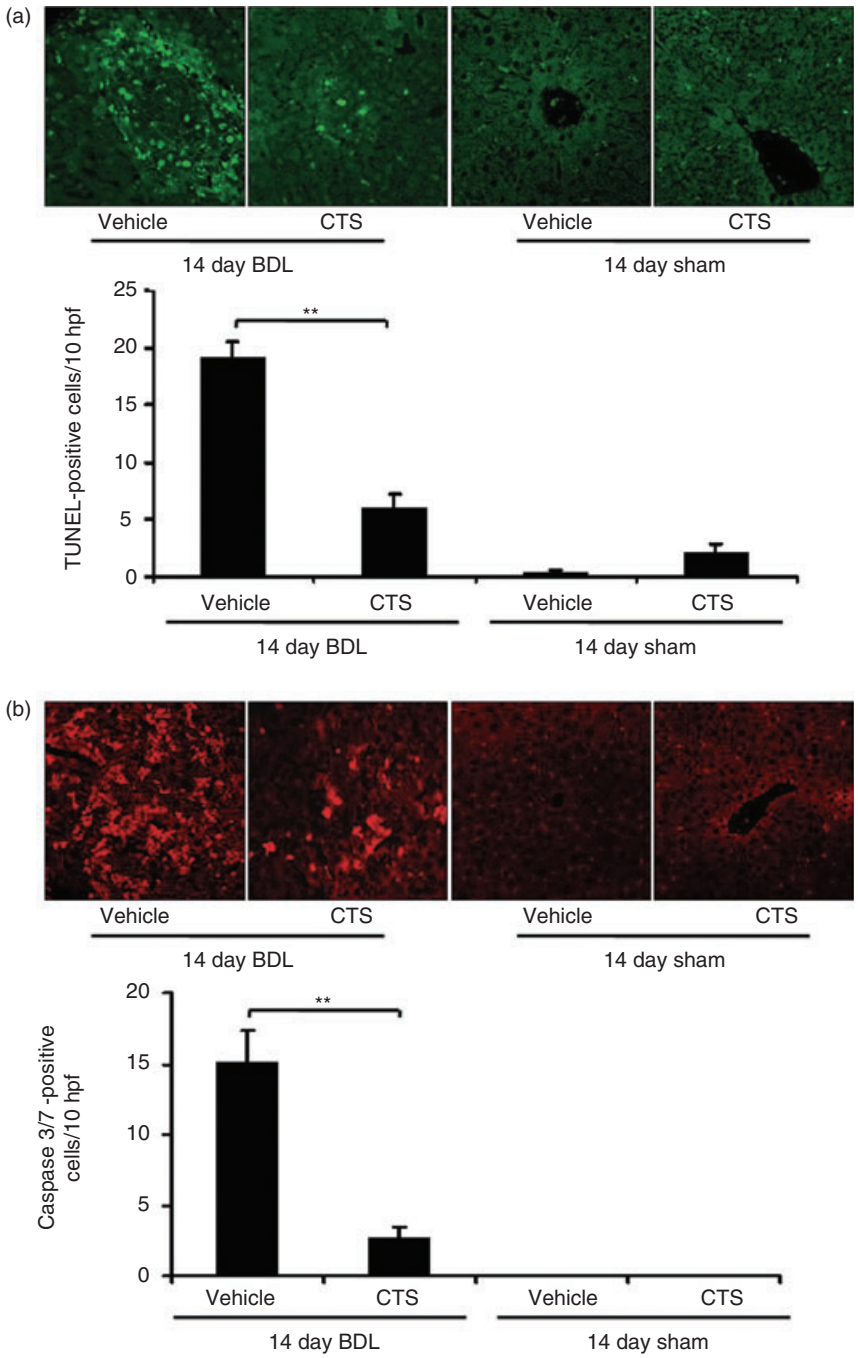

Figure 1 Hepatocyte apoptosis is reduced in 14 day bile duct ligation (BDL)-treated with CTS-1027. (a) The number of TUNEL-positive cells was quantitated and expressed as apoptotic cells/10 high-power fields (HPF). Data are from 10 independent animals per group and are expressed as the mean ± standard error, $^{*}P < 0.01$ by ANOVA for BDL mice treated with either the matrix metalloproteinase (MMP) inhibitor CTS-1027 or the vector carboxymethylcellulose (CMC). (b) Immunohistochemistry for the neo-epitopes of caspases 3/7 was performed. Again, data points represent experiments from 10 independent animals (BDL) or at least five sham animals (fewer used because no positive cells were seen in any sham animal) and bars are expressed as the mean ± standard error, $^{*}P < 0.01$ by ANOVA for BDL mice treated with either CTS-1027 or CMC.

Quantitation of these TUNEL-positive cells demonstrated a threefold decrease in BDL mice receiving CTS-1027 as compared to mice treated with vehicle (Fig. 1a). The activation of executioner caspases, especially caspases 3 and 7, is a biochemical hallmark of apoptosis.[15] Therefore, to further confirm hepatocyte apoptosis in animals following BDL, we next performed immunohistochemistry for activated caspases 3 and 7. Immunoreactive product was readily identified in liver tissues from mice following BDL, but not in sham-operated controls (Fig. 1b). Consistent with the TUNEL assay, BDL animals receiving CTS-1027 demonstrated a five-

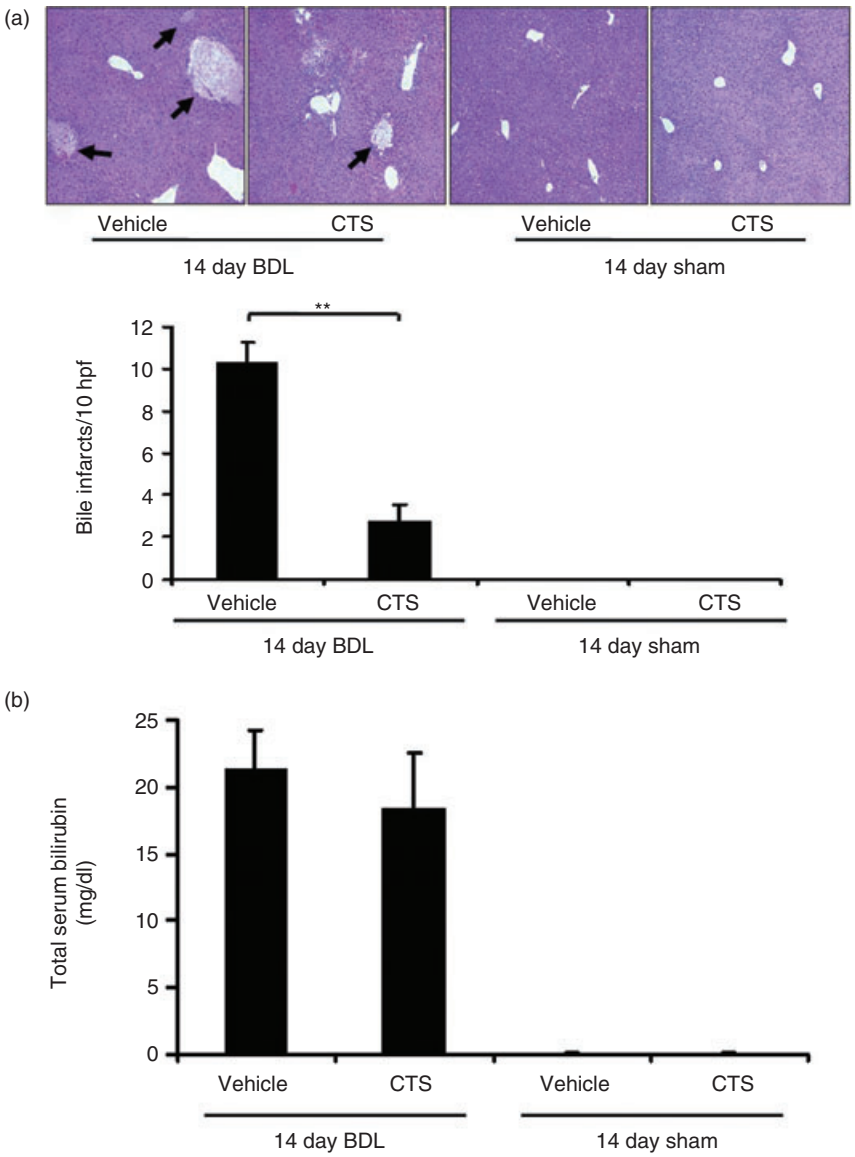

Figure 2 Cholestatic liver injury is attenuated in animals receiving CTS-1027 during bile duct ligation (BDL). (a) Representative photomicrographs of conventional hematoxylin–eosin-stained liver sections (original magnification ×20) are demonstrated. Liver specimens of BDL mice treated with the vector carboxymethylcellulose (CMC) displayed significant and extensive hepatocyte injury with bile infarcts (arrows), bile duct proliferation and portal edema. BDL-induced liver injury was markedly reduced in animals receiving the active drug CTS-1027, and absent in liver sections of sham-operated control mice. Bile infarcts (confluent foci of hepatocyte feathery degeneration caused by bile acid cytotoxicity) were quantified in all experimental groups ($n = 4$ for each condition). (b) Serum total bilirubin determinations are demonstrated 14 days after BDL ($n = 5$ for each condition).

fold decrease in the number of caspase 3/7-positive hepatocytes versus mice treated with the vehicle (Fig. 1b). Taken together, these data demonstrate that treatment with the MMP inhibitor CTS-1027 reduces hepatocyte apoptosis in the BDL mouse.

Features of cholestatic liver injury are significantly reduced in BDL mice treated with CTS-1027

To further examine the effects of CTS-1027 on liver injury during BDL, histopathological examination of liver specimens was performed. After 14 days of BDL, mice receiving vehicle displayed severe cholestatic hepatitis with evidence of widespread bile infarctions (Fig. 2a), a pathognomic feature of large bile duct obstruction in this animal.[16] This histopathological feature of obstructive cholestasis is recognized as confluent regions of hepatocellular degeneration and was reduced in liver specimens from animals receiving CTS-1027. Remarkably, these animals displayed almost intact liver morphology with excellent architectural preservation (Fig. 2a). This difference in cholestatic liver injury could not be ascribed to alterations in cholestasis as total bilirubin levels were almost identical in treated and untreated groups of animals (Fig. 2b). Interestingly, after 14 days of BDL, serum ALT values were not

different between the two groups (599 ± 68 vs 527 ± 89 U/L, $n = 8$ per group, $P > 0.05$). This observation is consistent with the fact that serum ALT values are a surrogate marker for liver injury and do not necessarily correlate with tissue injury as has been observed in human hepatitis C infection.[17] Taken together, these observations suggest MMP inhibition by CTS-1027 is hepato-protective during murine obstructive cholestasis.

Markers of hepatic fibrogenesis are attenuated in animals following BDL receiving CTS-1027

If the reduction of liver injury in BDL mice treated with CTS-1027 is significant, it should also translate into reduced hepatic fibrogenesis, a sequela of liver damage. Because stellate cells are the principal hepatic cell type responsible for collagen deposition in the liver,[18] we next quantified *α-SMA* transcripts, markers for stellate cell activation, by qRT–PCR. After 14 days of BDL, mRNA for *α-SMA* was reduced 60% in CTS-1027 treated animals as compared to those receiving vehicle (Fig. 3a). Immunoreactivity for *α-SMA*, which was increased in the sinusoid lining cells of BDL mice, was reduced in BDL mice treated with CTS-1027 (Fig. 3b). To ascertain if stellate cell activation was also associated with enhanced hepatic fibrogenesis, mRNA for hepatic *collagen 1α* (I) was quantified. Indeed, *collagen 1α* (I)

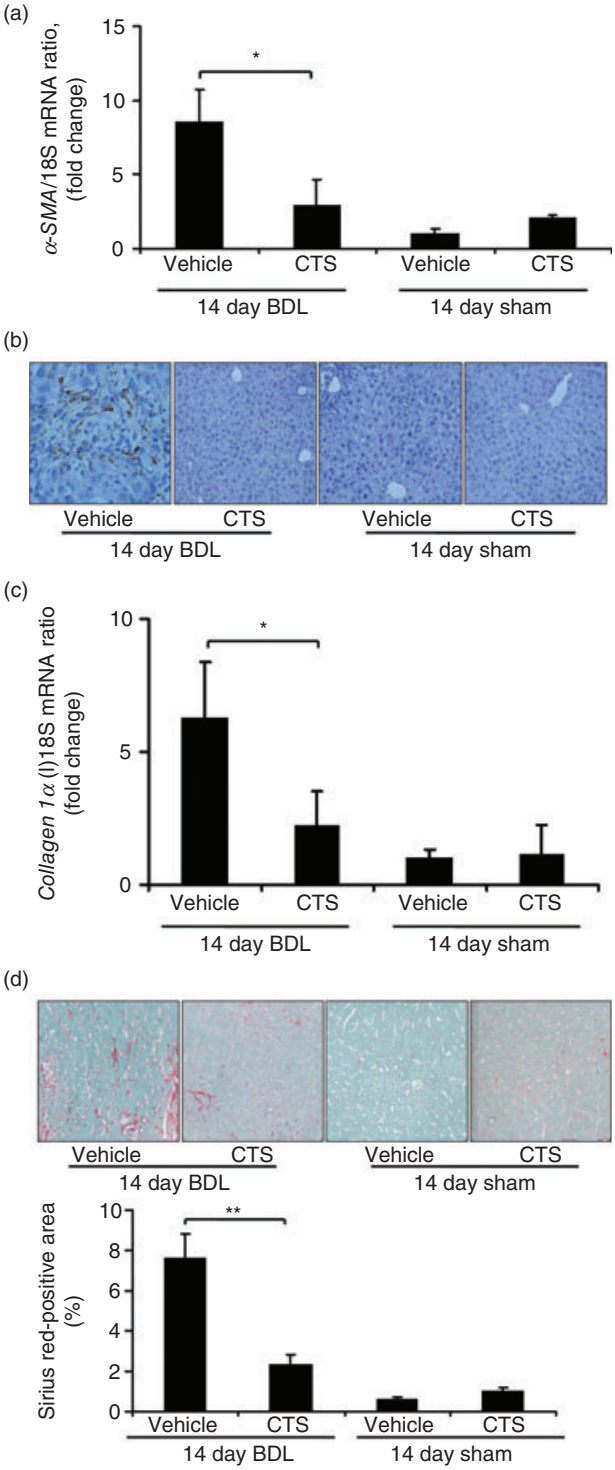

Figure 3 Hepatic fibrogenesis is reduced in bile duct ligation (BDL) animals upon treatment with CTS-1027. (a) α-Smooth muscle actin (*α-SMA*) and *collagen 1α* (I) mRNA expression, markers for stellate cell activation and hepatic fibrogenesis, were quantified by quantitative real-time polymerase chain reaction after 14 days of BDL. Data were obtained from 10 independent animals and are expressed as the mean ± standard error (*$P < 0.05$ by ANOVA). (b) Photomicrographs after immunohistochemistry for *α-SMA* following 14 days of BDL and gavage of either CTS-1027 or the vector CMC are depicted. (c) Expression of *collagen 1α* (I) mRNA was quantified by real time-PCR 14 days after BDL and treatment with either the MMP inhibitor CTS-1027 or the vector carboxymethylcellulose (CMC; *$P < 0.05$ by ANOVA, $n = 10$ for each group). (d) Sirius red staining, a chemical stain of collagen deposition in the liver, was performed 14 days after BDL. Collagen fibers stained with Sirius red were quantitated using digital image analysis. Representative photomicrographs of liver sections from each experimental condition are depicted (original magnification light microscopy ×40). Sirius red staining was quantitatively greater in mice treated with the vector CMC as compared to mice treated with CTS-1027 following BDL for 14 days (*$P < 0.05$ by ANOVA, $n = 10$ for each group).

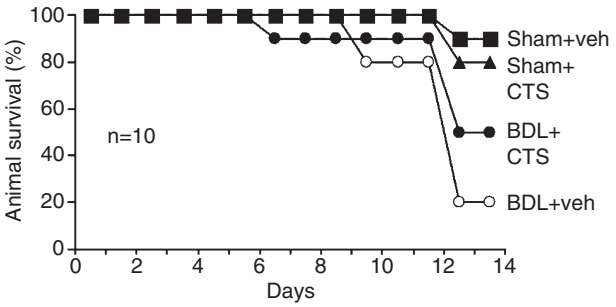

Figure 4 Overall animal survival following 14 days of bile duct ligation (BDL) is enhanced in mice upon treatment with the matrix metalloproteinase (MMP) inhibitor CTS-1027. Initially, on day 7 after BDL, 90% of animals treated with CTS-1027 were still alive whereas 100% of the mice receiving the vector carboxymethylcellulose (CMC) survived cholestatic liver injury. However, on day 13 after BDL, 50% of animals administered CTS-1027 by gavage were still alive compared to only 20% in the group treated with the vector CMC ($n = 10$ animals per group).

mRNA expression was decreased 60% in BDL animals following daily administration of CTS-1027 as compared to mice receiving the vehicle (Fig. 3c). Hepatic collagen protein deposition was further identified in liver specimens by Sirius red staining (Fig. 3d) and subjected to computer-assisted quantitative morphometry for quantification.[12] Collagen staining by Sirius red was decreased approximately 70% treated versus untreated mice in BDL mice (Fig. 3d). Collectively, these data suggest that, in BDL animals, stellate cell activation and hepatic fibrogenesis are attenuated by administration of the MMP inhibitor CTS-1027.

Overall animal survival following 14 days of BDL is improved in mice receiving the active drug CTS-1027

Given that liver injury and also hepatic fibrogenesis are significantly reduced in BDL mice treated with CTS-1027, we reasoned that animal survival should also be enhanced in this experimental group. Therefore, in our final study, we examined overall animal survival after BDL following treatment with CTS-1027 versus the CMC vehicle. By day 14 following BDL, 50% of the animals treated with CTS-1027 were alive as compared to only 20% of the mice receiving CMC (Fig. 4). Taken together, this study indicates that, during obstructive cholestasis, treatment with the MMP inhibitor CTS-1027 exerts a survival advantage.

DISCUSSION

IN THIS STUDY, we demonstrated that inhibition of MMP pharmacologically is beneficial in cholestatic liver injury. Cholestatic liver injury is likely mediated by a cascade of events. First, the acute retention of toxic bile acids promote hepatocyte injury, in part by death receptor-mediated processes.[19] This primary hepatocyte injury elicits a secondary phase of injury characterized by infiltration of inflammatory cells, activation of Kupffer cells and transformation of quiescent stellate cells to activated myofibroblasts. A component of the secondary phase of injury is due to MMP which induce remodeling of the extracellular matrix. This structural alteration of the liver further promotes liver injury and enhances hepatocyte apoptosis. Therefore, it is very likely in our current study that CTS-1027 inhibited the secondary injurious process in the liver. Interruption of this process attenuated further apoptosis and hepatic fibrosis. These data are consistent with the ability of MMP inhibition to decrease inflammation in TNF-α/galactosamine-treated mice.[6] Our study extends these observations by demonstrating an anti-fibrogenic effect of an MMP inhibitor in a subacute process of liver injury. There are no data to suggest that these agents alter the primary phase of bile acid-mediated liver injury. This is consistent with the elevated ALT values observed in both untreated and CTS-1027-treated BDL animals. Interestingly, in addition to their extracellular localization and function, MMP have been demonstrated to be present and functional in the cell nucleus,[20,21] including in the liver.[22] Further, they may have a role in apoptosis via their intracellular activity.[20–22] Because CTS-1027 is cell-permeable (2009, P.C. Contreras, Conatus Pharmaceuticals) we cannot exclude a role for intracellular MMP inhibition in the protection of hepatocytes from apoptosis.

Inhibition of MMP has been amply demonstrated to attenuate acute and chronic liver injury.[6,7] The current study extends these observations by employing the pharmacological compound CTS-1027 in a preclinical model of obstructive cholestasis. This model was selected because BDL mice consistently undergo hepatocyte apoptosis and hepatic fibrosis over a subacute time frame, permitting assessment of liver injury and remodeling. In this model, CTS-1027 was able to attenuate both hepatic injury and liver fibrosis. This model displays features similar to human liver injury where hepatocyte damage promotes inflammation, stellate cell activation and hepatic fibrogenesis. However, what is less clear, is what the effect of CTS-1027 would

be in a model where hepatic fibrosis is already established. One possibility is that CTS-1027 may limit further injury, as in the current model. Alternatively, because MMP-2, -8 and -13 also degrade collagen,[23] broad-spectrum inhibition of MMP could impair the resolution phase of hepatic fibrosis. This concept could not be explored in the BDL mouse model given the limited survival observed in these animals. Nonetheless, preventing further fibrogenesis and hepatic injury would have a salutary effect in human liver disease, even if the previously deposited collagen present in the matrix could not be degraded. Additional studies using models of chronic fibrosis and cirrhosis will be necessary to evaluate the effects of CTS-1027 in established fibrotic disease models. Based on these data, CTS-1027 warrants further study as a hepato-protective, anti-fibrogenic pharmacological agent in human liver disease. Indeed, a limited clinical trial with CTS-1027 in hepatitis C patients is currently ongoing.

ACKNOWLEDGMENTS

THE AUTHORS THANK Erin Nystuen-Bungum for her excellent secretarial assistance and James Tarara from the Division of Biochemistry and Molecular Biology (Mayo Clinic, Rochester) for quantitation of the Sirius red images. This study was supported by a fellowship grant from the Association for Scientific Research and Science at the Department of Gastroenterology and Hepatology, University Clinic Essen, Duisburg-Essen University, Germany (no. 45122) to A. K.; by grant no. DK 41876 from the National Institute of Health to G. J. G.; Conatus Pharmaceuticals; and the Mayo Foundation Rochester, Minnesota, USA.

REFERENCES

1 Friedman SL. Hepatic stellate cells: protean, multifunctional, and enigmatic cells of the liver. *Physiol Rev* 2008; **88:** 125–72.
2 Iredale JP. Cirrhosis: new research provides a basis for rational and targeted treatments. *BMJ* 2003; **327** (7407)**:** 143–7.
3 Elkington PT, O'Kane CM, Friedland JS. The paradox of matrix metalloproteinases in infectious disease. *Clin Exp Immunol* 2005; **142:** 12–20.
4 Roderfeld M, Hemmann S, Roeb E. Mechanisms of fibrinolysis in chronic liver injury (with special emphasis on MMPs and TIMPs). *Z Gastroenterol* 2007; **45:** 25–33.
5 Zhou XD. Recurrence and metastasis of hepatocellular carcinoma: progress and prospects. *Hepatobiliary Pancreat Dis Int* 2002; **1:** 35–41.
6 Wielockx B, Lannoy K, Shapiro SD *et al.* Inhibition of matrix metalloproteinases blocks lethal hepatitis and apoptosis induced by tumor necrosis factor and allows safe antitumor therapy. *Nat Med* 2001; **7** (11)**:** 1202–8.
7 Uchinami H, Seki E, Brenner DA, D'Armiento J. Loss of MMP 13 attenuates murine hepatic injury and fibrosis during cholestasis. *Hepatology* 2006; **44:** 420–9.
8 Miyoshi H, Rust C, Roberts PJ, Burgart LJ, Gores GJ. Hepatocyte apoptosis after bile duct ligation in the mouse involves Fas. *Gastroenterology* 1999; **117:** 669–77.
9 Kahraman A, Barreyro FJ, Bronk SF *et al.* TRAIL mediates liver injury by the innate immune system in the bile duct-ligated mouse. *Hepatology* 2008; **47:** 1317–30.
10 Natori S, Selzner M, Valentino KL *et al.* Apoptosis of sinusoidal endothelial cells occurs during liver preservation injury by a caspase-dependent mechanism. *Transplantation* 1999; **68:** 89–96.
11 Kurosawa H, Que FG, Roberts LR, Fesmier PJ, Gores GJ. Hepatocytes in the bile duct-ligated rat express Bcl-2. *Am J Physiol* 1997; **272** (6 Pt 1)**:** G1587–93.
12 Canbay A, Higuchi H, Bronk SF, Taniai M, Sebo TJ, Gores GJ. Fas enhances fibrogenesis in the bile duct ligated mouse: a link between apoptosis and fibrosis. *Gastroenterology* 2002; **123:** 1323–30.
13 Higuchi H, Bronk SF, Takikawa Y *et al.* The bile acid glycochenodeoxycholate induces trail-receptor 2/DR5 expression and apoptosis. *J Biol Chem* 2001; **276** (42)**:** 38610–8.
14 Arteel GE, Raleigh JA, Bradford BU, Thurman RG. Acute alcohol produces hypoxia directly in rat liver tissue in vivo: role of Kupffer cells. *Am J Physiol* 1996; **271** (3 Pt 1)**:** G494–500.
15 Cohen GM. Caspases: the executioners of apoptosis. *Biochem J* 1997; **326** (Pt 1)**:** 1–16.
16 Canbay A, Feldstein A, Baskin-Bey E, Bronk SF, Gores GJ. The caspase inhibitor IDN-6556 attenuates hepatic injury and fibrosis in the bile duct ligated mouse. *J Pharmacol Exp Ther* 2004; **308:** 1191–6.
17 Pradat P, Alberti A, Poynard T *et al.* Predictive value of ALT levels for histologic findings in chronic hepatitis C: a European collaborative study. *Hepatology* 2002; **36** (4 Pt 1)**:** 973–7.
18 Reeves HL, Friedman SL. Activation of hepatic stellate cells–a key issue in liver fibrosis. *Front Biosci* 2002; **7:** d808–26.
19 Faubion WA, Guicciardi ME, Miyoshi H *et al.* Toxic bile salts induce rodent hepatocyte apoptosis via direct activation of Fas. *J Clin Invest* 1999; **103:** 137–45.
20 Kwan JA, Schulze CJ, Wang W *et al.* Matrix metalloproteinase-2 (MMP-2) is present in the nucleus of cardiac myocytes and is capable of cleaving poly (ADP-ribose) polymerase (PARP) in vitro. *Faseb J* 2004; **18:** 690–2.
21 Limb GA, Matter K, Murphy G *et al.* Matrix metalloproteinase-1 associates with intracellular

organelles and confers resistance to lamin A/C degradation during apoptosis. *Am J Pathol* 2005; **166** (5)**:** 1555–63.
22 Si-Tayeb K, Monvoisin A, Mazzocco C *et al.* Matrix metalloproteinase 3 is present in the cell nucleus and is involved in apoptosis. *Am J Pathol* 2006 **169** (4)**:** 1390–401.
23 Cauwe B, Van den Steen PE, Opdenakker G. The biochemical, biological, and pathological kaleidoscope of cell surface substrates processed by matrix metalloproteinases. *Crit Rev Biochem Mol Biol* 2007; **42:** 113–85.